Research Paper

Author for correspondence:
Annemariè Avenant-Oldewage,
E-mail: aoldewage@uj.ac.za

CAMBRIDGE
UNIVERSITY PRESS

First isolation and scanning electron microscopy of haptoral sclerites of *Macrogyrodactylus* (Monogenea)

Mpho Maduenyane [ID], Quinton Marco Dos Santos [ID] and Annemariè Avenant-Oldewage [ID]

Department of Zoology, University of Johannesburg, Auckland Park, PO Box 524, Johannesburg, South Africa

Abstract

Macrogyrodactylus congolensis (Prudhoe, 1957) is one of six species of *Macrogyrodactylus*, all of which are endemic to Africa. This monogenean is a host-specific ectoparasite of the African sharptooth catfish, *Clarias gariepinus* (Burchell, 1822). It attaches to the host with a posterior haptor armed with sclerites. The specific morphology of sclerites is taxonomically significant and usually studied using light microscopy. The aim of the present study was to confirm the identification of macrogyrodactylid parasites using classic morphology (light microscopy of glycerine ammonium picrate mounted specimens) and molecular techniques (18S rDNA, ITS rDNA and cytochrome oxidase subunit 1 (COI) mtDNA). Additionally, the sclerites were accurately described with a technique not previously used for the genus, whereby haptoral sclerites were isolated by removing the encapsulating soft tissue with a digestion buffer and studied with scanning electron microscopy (SEM). Morphology and morphometry of studied specimens corresponded to available data for *M. congolensis*, confirming the identity of the parasite. All previous descriptions were summarized in a table and discrepancies discussed. Molecular analysis also confirmed the specimens to be *M. congolensis*, but ITS rDNA and COI mtDNA was more reliable than 18S rDNA in this regard. The isolation of haptoral sclerites and their study using SEM was successful, resolving the morphology of all sclerites. This study provided the first reconstruction of the haptor of a *Macrogyrodactylus* species following SEM analysis, as well as the first mtDNA for *M. congolensis*. Further study of isolated haptoral sclerites of other macrogyrodactylids is required to determine the full benefits of studying their isolated sclerites.

Introduction

Gyrodactylid flatworms of the genus *Macrogyrodactylus* Malmberg, 1957 represent the largest individuals of the family (Malmberg, 1957). They are host-specific and site-specific with many preferring the gills of their freshwater fish hosts and others occurring only on the skin and fins (Paperna, 1996). Site specificity in macrogyrodactylids was first reported by Arafa *et al.* (2013) in *Macrogyrodactylus congolensis* (Prudhoe, 1957) and *Macrogyrodactylus clarii* Gussev, 1961, which infect the skin and gills of *Clarias gariepinus* (Burchell, 1822), respectively. Arafa *et al.* (2013) noticed that neither of these species would attach when placed on the incorrect host tissue. Similar to all other monogeneans, *Macrogyrodactylus* parasites attach to their host using a haptor, which is also taxonomically significant (Khalil & Mashego, 1998). Malmberg (1957) described gyrodactylids of the genus *Macrogyrodactylus* to have 'one pair of anchors (hamuli) and 16 marginal fingers (hooks), two of which are triangular and point obliquely anteriad'. Haptoral structures in different *Macrogyrodactylus* species differ by size or shape (Malmberg, 1957; Khalil & Mashego, 1998; Přikrylová & Gelnar, 2008; Barson *et al.*, 2010). The male copulatory organ (cirrus) can also be used to distinguish *Macrogyrodactylus* species (Khalil & Mashego, 1998; N'Douba & Lambert, 1999). This organ develops at a particular stage of their life, consisting of a large spine surrounded by smaller spines which differ in number between species (Malmberg, 1957). For example, Khalil & Mashego (1998) recorded 10–11 small spines in *Macrogyrodactylus polypteri* Malmberg, 1957, 12–13 in *M. clarii*, and 14–15 small spines in *M. congolensis* and *Macrogyrodactylus karibae* Douëllou & Chishawa, 1995.

Taxonomic studies of monogeneans are traditionally based on the morphology of haptoral sclerites as they differ between species (Shinn *et al.*, 1993). This involved utilizing compound light microscopy to examine flat-mounted parasite specimens and measuring specific sclerites (Shinn *et al.*, 1993). However, several authors observed that in preparation of specimens for microscopical examination, the shape and or size of structures may be altered as a result of coverslip pressure or the type of fixative used, resulting in inconsistent measurements (Mo & Appleby, 1990; Shinn *et al.*, 1993; Fankoua *et al.*, 2017). To resolve this, Mo & Appleby

(1990) proposed the examination of isolated haptoral sclerites with scanning electron microscopy (SEM) by digesting the surrounding soft tissue with pepsin-based artificial gastric juices. Unfortunately, not all sclerites could be seen, hence Harris *et al.* (1999) removed the surrounding tissue with a digestion buffer containing tris hydrochloride, ethylenediaminetetraacetic acid, and sodium dodecyl sulphate (proteinase K as the active enzyme) as an alternative. Moreover, Hahn *et al.* (2011) digested the parasites on polylysine-coated slides to avoid loss of sclerites during digestion with a digestion buffer from a DNA extraction kit. Dos Santos & Avenant-Oldewage (2015) also reported using polylysine-coated slides to be effective for the isolation of sclerites in *Paradiplozoon vaalense* Dos Santos, Jansen van Vuuren & Avenant-Oldewage, 2013, but concavity slides were said to be more effective as digestion is restricted to the area of the concavity. The current study is the first to follow and modify this technique to examine isolated haptoral sclerites of a *Macrogyrodactylus* species with SEM.

Matejusová *et al.* (2003) presented the first molecular data for *Macrogyrodactylus* with the study on *M. polypteri*. To date, all valid species have been genetically characterized. The most common genetic markers used for DNA profiles of macrogyrodactylids are 18S and internal transcribed spacer (ITS; ITS1-5.8S-ITS2) regions of rDNA (Matejusová *et al.*, 2003; Barson *et al.*, 2010; Přikrylová *et al.*, 2013; Vanhove *et al.*, 2018; Truter *et al.*, 2021). *Macrogyrodactylus karibae* is the only species with additional 28S rDNA data, while cytochrome oxidase subunit 1 (COI) mtDNA data are available for *M. karibae*, *M. clarii* and *Macrogyrodactylus heterobranchii* N'Douba & Lambert, 1999, as well as hybrids of the latter two species (Matejusová *et al.*, 2003; Barson *et al.*, 2010; Vanhove *et al.*, 2018).

Materials and methods

Sample collection

Specimens of an unidentified monogenean parasite were removed from the skin of heavily infected *C. gariepinus* by performing a skin scrape with a glass microscope slide. These fish were acquired from a fish farm for another study and the parasites were unintentionally introduced into the research aquarium at the University of Johannesburg (Maduenyane *et al.*, 2022). Parasites were either mounted fresh as detailed below for light microscopy study, stored in 70% ethanol (Sigma-Aldrich, Germany) for examination with SEM, or stored in 96% ethanol for molecular analysis and study of isolated haptoral sclerites using SEM.

Light microscopy and morphometry

Specimens were individually placed on a microscope glass slide with a small volume of water and covered with a coverslip, the latter adhered to the slide by applying a small drop of nail varnish on each corner. Thereafter, filter paper was used to withdraw excess water by capillary action from the sides of the coverslip before a drop of glycerine ammonium picrate (GAP, one part of saturated ammonium picrate solution and one part of glycerine) (Malmberg, 1957) was placed at the edge of the coverslip, allowing it to slowly diffuse. Finally, all four sides of the coverslip were sealed with clear nail varnish. Specimens were initially observed using a Zeiss Stemi 350 stereomicroscope (Carl Zeiss, Germany), after which a Zeiss Axioplan 2 imaging light microscope with Axiovision 4.7.2 software was used to obtain photomicrographs using phase contrast. Haptoral sclerites (hamulus,

dorsal bar, ventral bar, long and short rods and marginal hooks) of GAP mounted specimens were measured as per Přikrylová & Gelnar (2008) and compared to measurements for *M. congolensis* by Khalil & Mashego (1998), El-Naggar *et al.* (1999), Přikrylová & Gelnar (2008), Barson *et al.* (2010) and Truter *et al.* (2021). Obtained photomicrographs were used to create line drawings of sclerites (shown in fig. 1) using CorelDRAW (Taylor & Karney, 1990), which were then compared to available illustrations (Khalil & Mashego, 1998; El-Naggar *et al.*, 1999; Přikrylová & Gelnar, 2008; Barson *et al.*, 2010; Truter *et al.*, 2021).

Morphology by SEM

For examination of isolated haptoral sclerites the methods of Nation (1983) and Dos Santos & Avenant-Oldewage (2015) were modified. Ten specimens previously preserved in 96% ethanol were re-hydrated, haptors removed with dissection needles, haptors individually placed on either a regular or concavity microscope slide, and digested in 1 µl of digestion buffer from a NucleoSpin® Tissue kit (Macherey-Nagel, Düren, Germany). The process was observed using a stereomicroscope. Once the soft tissues had partially digested, a coverslip was placed on top of the haptors that were digested on regular slides and affixed by the corners with nail vanish. After that 10 µl of distilled water was continually added at the sides to avoid crystallization of the digestion buffer. Once the digestion endpoint was observed (i.e., when only the sclerites remained), 10 µl of distilled water was added to one side of the coverslip and drawn out with a glass micropipette on the opposite side. This was repeated 3–4 times to ensure that all the digestion buffer and digested tissue was removed and only the sclerotized structures remained under the coverslip. Slides were then placed in a Sanpla dry keeper desiccator cabinet (Kita-Ku, Osaka, Japan) to dry overnight. Once dry, the coverslip was removed carefully from the microscope slide and repositioned upside down next to the dried area on the same slide. An Emscope SC500 sputter coater (Quorum Technologies, Lewes, UK) was used to coat the specimens with gold prior to examination using a TESCAN Vega 3 LMH SEM (Brno, Czech Republic) at 5 kV acceleration voltage.

DNA extraction and amplification

Genomic DNA was extracted from 10 parasite specimens stored in 96% ethanol using a NucleoSpin® Tissue kit (Macherey-Nagel, Düren, Germany). Three molecular markers (ITS rDNA, 18S rDNA and COI mtDNA) were used to study the identity and evolutionary history of the parasites. The internal transcribed spacer region of ribosomal DNA (ITS1 to 2) was amplified using the primers ITS1-fm (5′-TAGAGGAAGTACAAGTCG-3′) (Rubio-Godoy *et al.*, 2016) and ITS2R (5′-TCCTCCGCTTAGTGATA-3′) (Cunningham, 1997). A polymerase chain reaction (PCR) was conducted under the following conditions: 5 min at 95°C, then 30 cycles for 1 min at 95°C, 1 min at 48°C, 2 min at 72°C, and a final elongation of 10 min at 72°C. Secondly, a fragment of 18S rDNA was amplified using the primers 18S-E (5′-CCGAATT CGTCGACAACCTGGTTGATCCTGCCAGT-3′) and 18S-F (5′-CCAGCTTGATCCTTCTGCAGGTTC-3′) (Littlewood & Olson, 2001) with the following PCR conditions: 5 min at 95°C, then 30 cycles of 1 min at 95°C, 1 min at 58°C, 2 min at 72°C, and finally 10 min at 72°C. Finally, COI mtDNA was amplified using primers specifically designed for macrogyrodactylids, Macro_F1 (5′-CATAA GCGTGTWGGTGTTATTTATAG -3′) and Macro_R1 (5′-ACCT
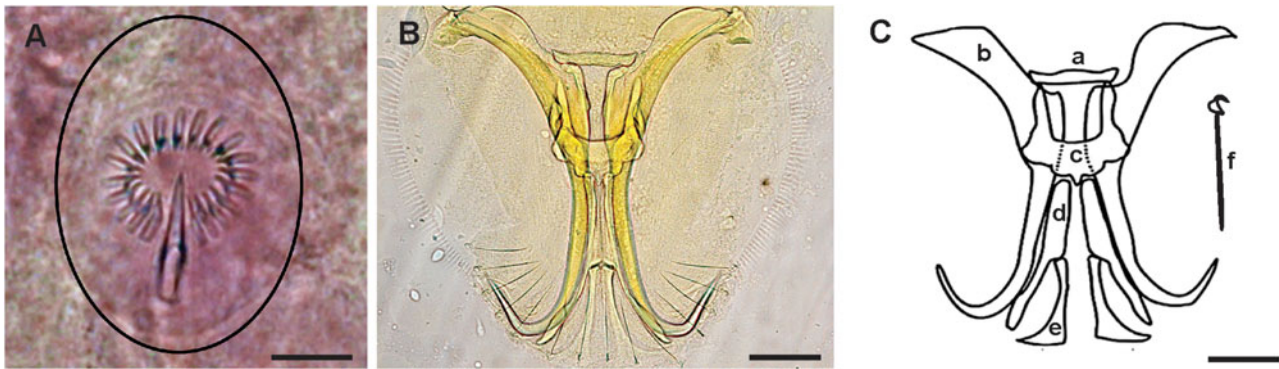
Fig. 1. (A) light micrograph of the male copulatory organ (encircled) consisting of one large spine surrounded by 20 small spines (scale bar = 20 µm); (B) light micrograph of a flattened haptor of *Macrogyrodactylus congolensis* (Prudhoe, 1957) in glycerine ammonium picrate (scale bar = 100 µm); and (C) line drawing of haptoral sclerites (scale bar = 100 µm). a - dorsal bar, b - hamulus, c - ventral bar, d - long ventral bar rod, e - short ventral bar rod, f - marginal hook.

CTGGATGTCCAAARAATC -3′) with the following PCR conditions: 5 min at 94°C, then 35 cycles of 45 s at 94°C, 45 s at 48°C, 2 min at 72°C, and finally 10 min at 72°C. Agarose gel (1%) impregnated with GelRed® (Biotium) was used for verification of successful amplification using an ultra-violet transilluminator (Labnet International, Inc.).

Sequencing and phylogeny

Amplicons were sequenced using standard BigDye chemistry and analysed on an ABI 3137 Automated Sequencer (Applied Biosystems, Foster City, CA, USA). Geneious Prime version 2019.1.1 (http://www.genious.com) was used to inspect, edit if required, merge and align obtained sequences. Resulting haplotypes were compared to sequences of other *Macrogyrodactylus* species from online data repositories. *Gyrdicotylus gallieni* Vercammen-Grandjean, 1960 was included as an outgroup for the ITS analysis, *Gyrodactylus carassii* (Malmberg, 1957) for the 18S analysis, and *Gyrodactylus parvae* You, Easy & Cone, 2008 for COI analysis; these species were chosen due to their proximity to obtained haplotypes as per Basic Local Alignment Search Tool (Altschul *et al.*, 1990). Genetic distances were determined using number of base pair differences and pairwise distances based on uncorrected *p*-distances in MEGA 7 (Tamura *et al.*, 2013). Phylogenetic topologies were constructed using maximum likelihood (ML) and Bayesian inference (BI) approaches. For ML, the Tamura 3-parameter model (Tamura, 1992) with Gamma distribution (5 categories (+G, parameter = 0.0500)) was selected for 18S as determined using the Model Selection tool in MEGA 7, while the Hasegawa–Kishino–Yano model (Hasegawa *et al.*, 1985) was selected for both ITS and COI analyses, with Gama distribution (5 categories (+G, parameter = 0.3323)) for ITS and evolutionarily invariable sites ([+I], 54.83%) for COI. The robustness of topologies was assessed using 1000 bootstrap replicates. For BI, BEAST v2.5.0 (Bouckaert *et al.*, 2014) was used with 10 million Markov chain Monte Carlo generations and the abovementioned models. Generated DNA sequences were submitted to GenBank under the following accession numbers: 18S rDNA (OM424629-33); ITS1 to 2 rDNA (OM426797-03); and COI mtDNA (OM456987-96).

Results and discussion

From the obtained light micrographs, it was observed that the features of the examined parasite specimens correspond with the diagnosis for *M. congolensis*. There was melanin deposition in the intestine of the parasites similar to what was observed by Khalil & Mashego (1998) for skin parasites of *C. gariepinus*. Both *M. karibae* and *M. clarii* have also been recorded from *C. gariepinus*, but lack pigmentation in the gut indicating that they are gill parasites (Khalil & Mashego, 1998). Arafa *et al.* (2013) observed the feeding mechanism of *M. congolensis* and stated that this parasite feeds on mucus and epithelia of the skin of its fish host, explaining the presence of darkly pigmented granules in the intestine of *M. congolensis*. These melanin granules have also been noted to be absorbed by the intestinal epithelium of the parasite (Maduenyane *et al.*, 2022)

The male copulatory organ consisted of one large spine surrounded by 20 small spines (*n* = 20). The first record of the number of spines for *M. congolensis* was by Prudhoe (1957) who recorded 15 small spines, followed by Douëllou & Chishawa (1995) who reported 14 small spines and Khalil & Mashego (1998) who recorded 14–15 small spines. Truter *et al.* (2021) recorded 18–20 small spines on the male copulatory organ of *M. congolensis* overlapping with the measurements obtained in the present study. These discrepancies in the number of small spines in *M. congolensis* need further investigation as this may indicate that this trait is unreliable, or the possibility of cryptic species.

Overall haptoral sclerite morphology of *M. congolensis* presented in El-Naggar *et al.* (1999), Khalil & Mashego (1998), Přikrylová & Gelnar (2008), Barson *et al.* (2010) and Truter *et al.* (2021) was identical to that of *Macrogyrodactylus* specimens from the current study (see line drawing and light micrograph in figs 1b, c and 2a–l). The haptor of *M. congolensis* (figs 1b, c and 2a–l, table 1) has two hamuli interconnected by a horizontal dorsal bar, a Y-shaped ventral bar consisting of two anterior lateral arms and a very short posterior central arm. Articulating the ventral bar is a pair of long ventral bar rods which are connected to a pair of short ventral bar rods. The anterior part of this short ventral bar rod has a narrow, rod-like anterior, that is made up of sclerotized material, but changes into a broad semi-sclerotized structure at the posterior end. The terminal end of the haptor is armed with marginal hooklets comprising a hook handle attached to a sickle. All specimens were armed with 16 marginal hooklets of similar morphology, 14 at the posterior end of the haptor and two extending from the anterolateral lobes.

The construction of the short ventral bar rod from specimens of the present study (fig. 2a–l) corresponded with that presented
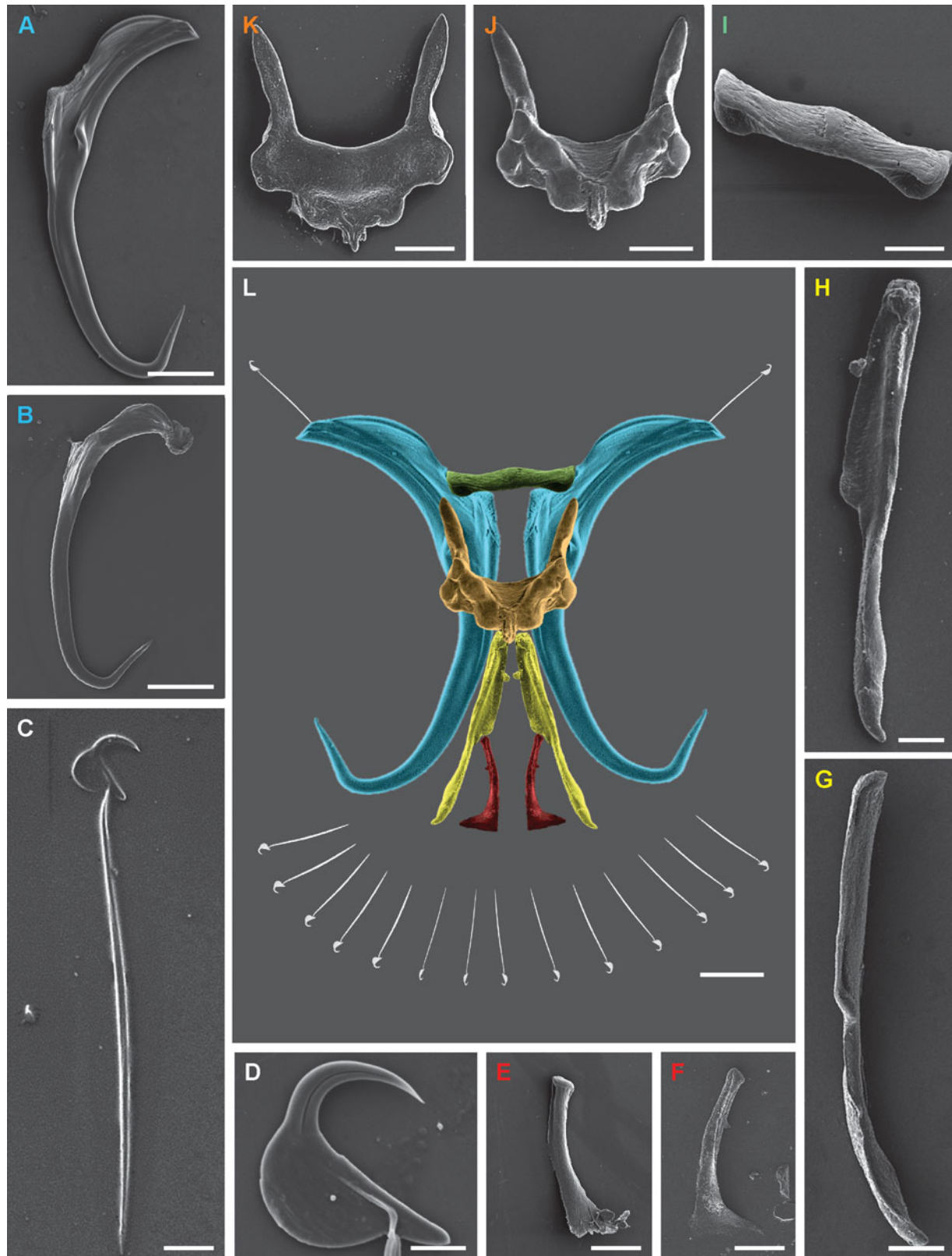
Fig. 2. Scanning electron micrographs showing different haptoral sclerites of *Macrogyrodactylus congolensis*. (a) dorsal side of hamulus (scale bar = 100 μm); (b) ventral side of hamulus (scale bar = 100 μm); (c) marginal hook (scale bar = 20 μm); (d) enlarged view of the hook sickle (scale bar = 5 μm); (e) dorsal side of short ventral bar rod (scale bar = 20 μm); (f) ventral side of short ventral bar rod (scale bar = 20 μm); (g) side view of the long ventral bar rod (scale bar = 100 μm); (h) dorsal aspect of long ventral bar rod (scale bar = 50 μm); (i) dorsal aspect of the dorsal bar (scale = 50 μm); (j) ventral aspect of the ventral bar (scale bar = 50 μm); (k) dorsal aspect of the ventral bar (scale bar = 50 μm); and (l) a coloured reconstruction of the haptor using the scanning electron microscopy images of isolated haptoral sclerites showing pair of hamuli, dorsal bar, ventral bar, a pair of long ventral bar rods, a pair of short ventral bar rods and 16 marginal hooks (14 at the margins of the haptor and 2 pointing anteriad at each side of the haptor) (scale bar = 100 μm). Colours of the labels correspond with the structure in the reconstructed haptoral sclerites.

Table 1. Measurements (all in μm) of haptoral sclerites of specimens from the present study (boldface type) in comparison to known data of the three *Macrogyrodactylus* species parasitizing *Clarias gariepinus*.

| | | *Macrogyrodactylus karibae* **Douëllou & Chishawa, 1995** | | *Macrogyrodactylus clarii* Gussev, 1661 | | | *Macrogyrodactylus congolensis* (**Prudhoe, 1957**) | | | | | | | |
		Khalil & Mashego (1998)	Barson et al. (2010) n = 6	El-Naggar & Serag (1987) n = 10	Khalil & Mashego (1998)	Barson et al. (2010) n = 10	Přikrylová & Gelnar (2008) n = 3	El-Naggar et al. (1999)	Khalil & Mashego (1998)	Barson et al. (2010) n = 723	Truter et al. (2021) South Africa n = 25	Truter et al. (2021) South Africa n = 2	Truter et al. (2021) Zimbabwe n = 2	Present study n = 20
hamulus	total length	296–375	312 (292–330)	385 (376–392)	437–453	436 (374–475)	–383 (381–385)	365 (315–415)	490–530	421 (385–481)	456 (390–537)	399 (391–407)	430 (419–440)	**471 ± 19 (432–499)**
	root length	125–156	144 (114–160)	178 (176–184)	193–203	191 (135–238)	154 (145–165)	–	251–287	175 (153–203)	203 (166–272)	178 (177–179)	175 (165–186)	**1s1 ± 19 (160–204)**
	shaft length	251–296	259 (245–273)	–	381–406	380 (350–457)	306 (299–313)	–	296–312	334 (310–361)	368 (310–431)	325 (318–332)	339 (339)	**371 ± 16 (30–407)**
	point length	68–93	83 (74–90)	120 (112–128)	131–140	120 (108–136)	101 (99–103)	–	80–109	99 (93–103)	111 (94–131)	98 (95–102)	106 (105–107)	**90 ± 8 (81–109)**
dorsal bar[a]	length	68–78	17 (15–20)	34(32–36) *	68–75*	17(14–20) *	14 (13–15)	82 (72–90)	15–18	18 (16–20)	22 (16–25)	20	20 (19–22)	**18 ± 1 (15–20)**
	width	15–21	88(80–92)	–	15–18*	82 (73–92)	90 (88–94)	16 (13–20)	109–125	98 (93–103)	115 (97–140)	103	101	**115 ± 11 (107–131)**
ventral bar	total length	84–111	104 (94–113)	110 (104–116)	140–147	148 (137–172)	129 (124–134)	135 (82–153)	140–162	143 (131–150)	156 (134–170)	147 (146–148)	147 (145–150)	**155 ± 11 (135–185)**
	maximum width	78–111	109 (99–120)	106 (96–112)	109–118	138 (122–157)	112 (109–114)	90 (45–110)	120–134	124 (118–130)	133 (110–153)	129 (126–133)	124 (122–125)	**134 ± 5 (127–155)**
	length of anterior lateral arm	21–31	18 (17–20)	–	21–31	29 (17–38)	65 (58–71)	–	84–93	90 (82–118)	93 (84–101)	85 (84–85)	85 (82–88)	**89 ± 6 (80–103)**
	length of the posterior central arm	24–40	42 (37–47)	–	46–65	69 (61–85)	9 (8–10)	–	12–15	7 (6–9)	9 (5–13)	6 (5–7)	8 (7–10)	**19 ± 3 (13–23)**
ventral bar rods	length of the long rod	–	182 (177–189)	–	–	191 (177–207)	217 (211–224)	–	–	236 (217–254)	254 (222–306)	239 (230–248)	238 (237–239)	**258 ± 8 (240–288)**
	length of the short rod	–	114 (101–125)	–	–	147 (141–157)	127 (120–137)	–	–	132 (126–141)	141 (118–179)	136 (134–137)	129 (118–140)	**137 ± 11 (120–179)**

(*Continued*)

Table 1. (*Continued.*)

		Macrogyrodactylus karibae **Douëllou & Chishawa, 1995**		*Macrogyrodactylus clarii* Gussev, 1661			*Macrogyrodactylus congolensis* (**Prudhoe, 1957**)							
		Khalil & Mashego (1998)	Barson *et al.* (2010) *n* = 6	El-Naggar & Serag (1987) *n* = 10	Khalil & Mashego (1998)	Barson *et al.* (2010) *n* = 10	Přikrylová & Gelnar (2008) *n* = 3	El-Naggar *et al.* (1999)	Khalil & Mashego (1998)	Barson *et al.* (2010) *n* = 723	Truter *et al.* (2021) South Africa *n* = 25	Truter *et al.* (2021) South Africa *n* = 2	Truter *et al.* (2021) Zimbabwe *n* = 2	Present study *n* = 20
marginal hooks	total length	68–78	80 (72–84)	–	109–125	115 (104–132)	95	85 (66–82)	81–87	97 (95–101)	104 (96–124)	95 (91–100)	96 (91–101)	**99 ± 5 (87–107)**
	length of handle	–	69 (61–74)	–	–	96 (88–112)	82.7 (78–86)	73 (56–80)	–	85 (84–89)	92 (83–114)	84 (80–87)	83 (77–89)	**88 ± 5 (77–99)**
	length of sickle	–	11 (11–12)	–	–	19 (17–21)	11 (10–12)	10 (8–10)	–	11 (11–12)	12 (10–14)	11	5 (11)	**13 ± 2 (8–17)**
	proximal width of sickle	–	9 (9–10)	–	–	14 (13–17)	10 (9– 11)	–	–	11 (10–12)	11 (8–14)	9 (8–9)	5 (10–10)	**8 ± 2 (5–14)**
pharynx anterior region	length	–	–	–	–	–	–	115 (90–165)	–	–	–	–	–	**62 ± 19 (48–100)**
	width	–	–	–	–	–	–	160 (90–195)	–	–	–	–	–	**108 ± 23 (65–145)**
pharynx posterior region	length	–	–	–	–	–	–	100 (90–195)	–	–	–	–	–	**74 ± 16 (48–100)**
	width	–	–	–	–	–	–	212 (180–270)	–	–	–	–	–	**127 ± 12 (114–150)**
testis	length	–	–	–	–	–	–	173 (90–210)	–	–	–	–	–	**98 ± 17 (74–119)**
	width	–	–	–	–	–	–	56 (54–210)	–	–	–	–	–	**82 ± 19 (48–116)**

n = number of measurements.
[a]* indicate that dorsal bar is divided.

in Khalil & Mashego (1998), Přikrylová & Gelnar (2008), Barson et al. (2010) and Truter et al. (2021) for M. congolensis, but was dissimilar to that provided in El-Naggar et al. (1999). According to El-Naggar et al. (1999), the short ventral bar rod was described and illustrated as an 'inverted Y-shaped accessory sclerite', as opposed to the wedge shape in the current and all other previous studies. It is possible that El-Naggar et al. (1999) may have misinterpreted the structure of the sclerite due to the use of light microscopy. This emphasizes the importance of the isolation and subsequent SEM study of sclerites.

Comparing the two other species of Macrogyrodactylus parasitizing C. gariepinus, the dorsal bar in M. clarii is divided into two small sclerites articulating with each other medially (Gussev, 1961; El-Naggar & Serag, 1987; El-Naggar et al., 2020), while this structure is fused, forming a single continuous sclerite in M. congolensis (figs 1b, c and 2i, l) and M. karibae (Prudhoe, 1957; Khalil & Mashego, 1998). Furthermore, the dorsal bar has a small central ridge at the top in M. karibae. Another distinction is that in M. karibae and M. clarii the ventral bar has relatively short anterior lateral arms and an elongated posterior central arm, with the latter much longer in M. clarii (El-Naggar & Serag, 1987; Khalil & Mashego, 1998; El-Naggar et al., 1999; El-Naggar et al., 2020).

Although the morphology of the haptoral sclerites (fig. 2a–l) was mostly identical to those presented in other studies (El-Naggar et al., 1999; Khalil & Mashego, 1998; Přikrylová & Gelnar, 2008; Barson et al., 2010; Truter et al., 2021), the obtained haptoral sclerite morphometry showed variation. Sclerite measurements for M. congolensis provided by Khalil & Mashego (1998) were smaller than those obtained in the present study, except for dorsal bar length and width, as well as the hamulus total length, which was larger in the specimens studied by Khalil & Mashego (1998). Moreover, when measurements obtained in the current study (table 1) were compared to those presented by Přikrylová & Gelnar (2008) for M. congolensis, there were differences in measurements of the hamulus root and shaft lengths, dorsal bar width and the long ventral bar rod length, which were larger in the present study while the measurements of the other sclerites overlapped. Haptoral sclerite measurements presented in Barson et al. (2010) overlap greatly with those obtained in the present study, with variation only observed in measurements of the dorsal and ventral bar width, hamulus shaft length, posterior central arm length and the length of the long ventral bar rod. In comparison to sclerite measurements by Truter et al. (2021) the total length of the hamulus as well as the total length of the marginal hooks were larger than in the present study. Measurements of the dorsal bar overlapped with other studies. Overall, the majority of sclerite measurements from the present study correlated with those in other studies (table 1).

Additional features that were considered for morphological comparison were the size and shape of marginal hooks as proposed by Přikrylová & Gelnar (2008). As can be seen in table 1, descriptions before 2008 do not include measurements of the marginal hook total length, hook handle, proximal sickle width and sickle length. Moreover, the obtained measurements of the pharynx and testis were compared to those in El-Naggar et al. (1999). Measurements of the anterior and posterior region of the pharynx had similar features in the present study and that by El-Naggar et al. (1999) as the posterior region of the pharynx was larger than the anterior region. Specimens from the current study had a smaller anterior and posterior pharynx than those

in El-Naggar et al. (1999). The testis as reported by El-Naggar et al. (1999) was larger than those from the present study; however, the testis was found to be longer than wide in both studies. Therefore, all morphological data support that the specimens studied here are M. congolensis and it is also the only Macrogyrodactylus species infecting the skin of C. gariepinus.

Five informative sequences of 18S rDNA were obtained representing two haplotypes. The two haplotypes only differed at one site which was polymorphic in the first haplotype and resolved in the second. The obtained alignment with available data was 1942 base pairs (bp) with 1809 bp conserved, 121 bp variable, and 26 bp parsimony informative. The first haplotype was identical (online supplementary table S1) to sequence data for both M. congolensis (HF548680) and M. karibae (MG973078), with the second haplotype only differing from these sequences by 0.05% (1 bp). As such, using the available 18S rDNA data for Macrogyrodactylus, the specimens could not be positively identified. Based on available 18S rDNA for macrogyrodactylids (excluding hybrids), no intraspecific ranges could be calculated, but the very low interspecific range of 0–2.08% (0–38 bp) indicates a highly conserved 18S rDNA region. Seven viable sequences for ITS rDNA were obtained, displaying four haplotypes. Similar to 18S rDNA, the haplotypes only differed in the resolution of polymorphic sites, with 9–18 polymorphic sites depending on the haplotype. The obtained alignment with available data was 922 bp with 545 bp conserved, 327 bp variable and 125 bp parsimony informative. Irrespective the number of polymorphic sites, all haplotypes were identical to that of M. congolensis from South Africa (MZ869848), only differing by 0.63–0.87% (4–7 bp) and 0.75–1.11% (6–9 bp) from the same species in Senegal (GU252717) and Kenya (GU252716), respectively (online supplementary table S2). Based on available ITS rDNA data for macrogyrodactylids (excluding hybrids), an intraspecific range of 0–1.95% (0–14 bp) and an interspecific range of 0.83–23.01% (6–156 bp) was observed. There is a large overlap in these ranges, primarily due to the proximity of M. clarii and M. heterobranchii which are known to hybridize (Barson et al., 2010) and secondarily the proximity of M. congolensis and M. karibae. Distances of ITS rDNA of studied material to available data for M. congolensis are more likely to represent intraspecific than interspecific variation, thus confirming the identity of the specimens. The larger distance between specimens from South Africa to those in Kenya and Senegal, and the similarity between data from the latter two countries, may indicate a correlation between geographical proximity and genetic variability, but this needs further investigation.

Sequence data for COI mtDNA was obtained from all studied specimens, representing two haplotypes. The two haplotypes only differed at one site. The obtained alignment with available data was 641 bp with 413 bp conserved, 228 bp variable and 147 bp parsimony informative. Based on available COI mtDNA for macrogyrodactylids (excluding hybrids), no intraspecific ranges could be calculated, but an interspecific range of 4.91–18.93% (21–81 bp) was observed (online supplementary table S3). The two haplotypes of COI mtDNA only differed by 0.23% (1 bp) and were 16.82–19.63% (72–103 bp) from other macrogyrodactylid data. This indicated that the variation observed is likely intraspecific, and the M. congolensis is distinct from other species based on COI mtDNA. The current study presents the first mitochondrial data for M. congolensis. It is noteworthy that M. congolensis is more distant to M. karibae using COI mtDNA (16.82–17.06%; 72–73 bp) than the latter species to either M. clarii

(14.49%; 62 bp) or *M. heterobranchii* (14.49%; 62 bp). This is in contrast to the results from rDNA analyses and warrants further investigation. However, the close relation of *M. clarii* and *M. heterobranchii* in rDNA analyses is mirrored in the mtDNA analyses of these species (4.91%; 21 bp), as well as their hybrids (0.23%– 5.14%; 1–22 bp). No mtDNA data are currently available for *M. polypterid* or *M. simentiensis*.

Phylogenies based on both 18S and ITS rDNA produced similar topologies (online supplementary figs S1 and S2). In both cases, the sequence data from the present study grouped with available data for *M. congolensis*. For ITS rDNA, *M. congolensis* formed a sister clade to *M. karibae*, while for 18S rDNA these two species formed a single clade. In both topologies, the clade containing *M. congolensis* and *M. karibae* was sister to a clade containing *M. clarii*, *M. heterobranchii* and the hybrids of these two species. Interestingly, in the 18S rDNA phylogeny, *M. simentiensis* grouped with hybrids of *M. clarii* and *M. heterobranchii*, as opposed to its placement in the ITS rDNA topology where it is basal to the aforementioned clades. Finally, *M. polypteri* is basal to all other macrogyrodactylids in both analyses. The phylogeny based on COI mtDNA differs greatly from this based on rDNA in that *M. congolensis* groups sister to all other macrogyrodactylid data (online supplementary fig. S3). As such, *M. karibae* groups with *M. clarii* and *M. heterobranchii* (and their hybrids). This may indicate that COI mtDNA is not suitable to infer phylogenetic relationships of macrogyrodactylid taxa, but it does show promise for species identification.

The isolation of haptoral sclerites resolved the morphology of some sclerites, alongside the first reconstruction of the haptor of a *Macrogyrodactylus* species using SEM. 18S rDNA did not show any distinction between *M. karibae* and *M. congolensis*. However, these species are morphologically distinct, indicating that 18S rDNA is not suitable to distinguish closely related taxa due its conserveness. Based on ITS rDNA and COI mtDNA, *M. congolensis* and *M. karibae* could be distinguished indicating the usefulness of these markers. Further research regarding molecular analysis and the suitability of additional markers for species identification and phylogenetic studies, as well as further study of isolated haptoral sclerites of other macrogyrodactylids, is required.

References

Altschul SF, Gish W, Miller W, Myers EW and Lipman DJ (1990) Basic local alignment search tool. *Journal of Molecular Biology* **215**(3), 403–410.

Arafa SZ, El-Naggar MM and Kearn GC (2013) Ultrastructure of the digestive system and experimental study of feeding in the monogenean skin and fin parasite *Macrogyrodactylus congolensis*. *Acta Parasitologica* **58**(4), 420–433.

Barson M, Přikrylová I, Vanhove MPM and Huyse T (2010) Parasite hybridization in *Macrogyrodactylus* spp. (Monogenea, Platyhelminthes) signals historical host distribution. *Parasitology* **137**(10), 1585–1595.

Bouckaert R, Heled J, Kühnert D, Vaughan T, Wu CH, Xie D, Suchard MA, Rambaut A and Drummond AJ (2014) BEAST 2: A software platform for Bayesian evolutionary analysis. *PLOS Computational Biology* **10**, e1003537.

Cunningham CO (1997) Species variation within the internal transcribed spacer (ITS) region of *Gyrodactylus* (Monogenea: Gyrodactylidae) ribosomal RNA genes. *Journal of Parasitology* **83**(2), 215–219.

Dos Santos QM and Avenant-Oldewage A (2015) Soft tissue digestion of *Paradiplozoon vaalense* for SEM of sclerites and simultaneous molecular analysis. *Journal of Parasitology* **101**(1), 94–97.

Douëllou L and Chishawa AMM (1995) Monogeneans of three siluriform fish species in Lake Kariba, Zimbabwe. *Journal of African Zoology* **109**(2), 99–115.

El-Naggar MM and Serag HM (1987) Redescription of *Macrogyrodactylus clarii* Gussev 1961, a monogenean gill parasite of *Clarias lazera* in Egypt. *Arab Gulf Journal of Scientific Research, B (Agriculture and Biological Sciences)* **5**, 257–271.

El-Naggar MM, Kearn GC, Hagras AE and Arafa SZ (1999) On some anatomical features of *Macrogyrodactylus congolensis*, a viviparous monogenean ectoparasite of the catfish *Clarias gariepinus* from Nile water. *Journal of the Egyptian–German Society of Zoology* **29**(1), 1–24.

El-Naggar MM, Arafa SZ, El-Abbassy SA, Kearn GC and Cable J (2020) Light and transmission electron microscopy of the haptoral sclerites of the monogenean gill parasite *Macrogyrodactylus clarii*. *Parasitology Research* **119**(12), 4089–4101.

Fankoua SO, Nyom BAR, Bahanak DND, Bilong Bilong CF and Pariselle A (2017) Influence of preservative and mounting media on the size and shape of monogenean sclerites. *Parasitology Research* **116**, 2277–2281.

Gussev AB (1961) A viviparous monogenetic trematode from freshwater basins of Africa. *Doklady Akademy Nauka SSSR* **136**, 490–493.

Hahn C, Bakke TA, Bachmann L, Weiss S and Harris PD (2011) Morphometric and molecular characterization of *Gyrodactylus teuchis* Lautraite, Blanc, Thiery, Daniel & Vigneulle, 1999 (Monogenea: Gyrodactylidae) from an Austrian brown trout population. *Parasitology International* **60**(4), 480–487.

Harris PD, Cable J, Tinsley RC and Lazarus CM (1999) Combined ribosomal DNA and morphological analysis of individual gyrodactylid monogeneans. *Journal of Parasitology* **85**(2), 188–191.

Hasegawa M, Kishino H and Yano T (1985) Dating the human–ape split by a molecular clock of mitochondrial DNA. *Journal of Molecular Evolution* **22**(2), 160–174.

Khalil LF and Mashego SN (1998) The African monogenean gyrodactylid genus *Macrogyrodactylus* Malmberg, (1957), and the reporting of three species of the genus on *Clarias gariepinus* in South Africa. *Onderstepoort Journal of Veterinary Research* **65**(4), 223–231.

Littlewood DTJ and Olson PD (2001) Small subunit rDNA and the platyhelminthes: Signal, noise, conflict and compromise. pp. 262–278. In Littlewood DTJ and Bray RA (Eds) *Interrelationships of the Platyhelminthes*. London, Taylor & Francis.

Maduenyane M, Dos Santos QM and Avenant-Oldewage A (2022) Light and scanning electron microscopy of the effects of *Macrogyrodactylus congolensis* (Prudhoe, 1957) on the skin of the African sharptooth catfish *Clarias gariepinus* (Burchell, 1822). *Journal of Fish Diseases*, 1–8. doi:10.1111/jfd.13584

Malmberg G (1957) On the new genus of viviparous monogenetic trematodes. *Arkiv for Zoologi* **10**, 317–329.

Matejusová I, Gelnar M, Verneau O, Cunningham CO and Littlewood DT (2003) Molecular phylogenetic analysis of the genus *Gyrodactylus* (Platyhelminthes: Monogenea) inferred from rDNA ITS region: Subgenera versus species groups. *Parasitology* **127**(6), 603–611.

Mo TA and Appleby C (1990) A special technique for studying haptoral sclerites of monogeneans. *Systematic Parasitology* **17**(2), 103–108.

Nation JL (1983) A new method using hexamethyldisilazane for preparation of soft insect tissues for scanning electron microscopy. *Stain Technology* **58**(6), 347–351.

N'Douba V and Lambert A (1999) A new *Macrogyrodactylus* (Monogenea, Gyrodactylidae) parasite of *Heterobranchus longifilis* Valenciennes, 1840 (Teleostei, Siluriformes) in Côte d'Ivoire. *Zoosystema* **21**(1), 7–11.

Paperna I (1996) *Parasites, infections and diseases of fishes in Africa: An update*. CIFA Technical Paper 3l. FAO, Rome, Italy.

Přikrylová I and Gelnar M (2008) The first record of *Macrogyrodactylus* species (Monogenea, Gyrodactylidae) on freshwater fishes in Senegal with the description of *Macrogyrodactylus simentiensis* sp. nov., a parasite of *Polypterus senegalus* Cuvier. *Acta Parasitologica* **53**(1), 1–8.

Přikrylová I, Vanhove MPM, Janssens SB, Billeter PA and Huyse T (2013) Tiny worms from a mighty continent: high diversity and new phylogenetic lineages of African monogeneans. *Molecular Phylogenetics and Evolution* **67**(1), 43–52.

Prudhoe S (1957) Trematoda. *Parc National de L'Upemba*. I Mission G F de Witte en collaboration avec Adam W, Janssens A, Van Meel L et Verheyen R (1946–1949) **48**, 1–28.

Rubio-Godoy M, Razo-Mendivil U, Garcia-Vasquez A, Freeman M, Shinn A and Paladini G (2016) To each his own: no evidence of gyrodactylid parasite host switches from invasive poecilid fishes to *Goodea atripinnis* Jordan (Cyprinodontiformes: Goodeidae), the most dominant endemic freshwater goodeid fish in the Mexican highlands. *Parasites & Vectors* **9**(1), 604–626.

Shinn AP, Gibson DI and Sommerville C (1993) An SEM study of the haptoral sclerites of the genus *Gyrodactylus* Nordmann, 1832 (Monogenea) following extraction by digestion and sonication technique. *Systematic Parasitology* **25**(2), 135–144.

Tamura K (1992) Estimation of the number of nucleotide substitutions when there are strong transition-transversion and G + C-content biases. *Molecular Biology and Evolution* **9**(4), 678–687.

Tamura T, Stecher G, Peterson D, Filipski A and Kumar S (2013) MEGA 7: Molecular evolutionary genetics analysis version 6.0. *Molecular Biology and Evolution* **30**(12), 2725–2729.

Taylor M and Karney J (1990) *CorelDRAW quick reference*. Indianapolis, USA, Que Corp.

Truter M, Acosta AA, Weyl OLF and Smit NJ (2021) Novel distribution records and molecular data for species of *Macrogyrodactylus* Malmberg, 1957 (Monogenea: Gyrodactylidae) from *Clarias gariepinus* (Burchell) (Siluriformes: Clariidae) in southern Africa. *Folia Parasitologica* **68**, 027.

Vanhove MPM, Briscoe AG, Jorissen MWP, Littlewood DTJ and Huyse T (2018) The first next-generation sequencing approach to the mitochondrial phylogeny of African monogenean parasites (Platyhelminthes: Gyrodactylidae and Dactylogyridae). *BMC Genomics* **19**(1), 1–17.